

Available online at www.sciencedirect.com

ScienceDirect

www.elsevier.com/locate/jes

The balance of acidity and redox capability over modified CeO₂ catalyst for the selective catalytic reduction of NO with NH₃

Zhihua Lian¹, Wenpo Shan¹, Meng Wang¹, Hong He^{1,2,3,*}, Qingcai Feng^{2,*}

1. Center for Excellence in Regional Atmospheric Environment and Key Laboratory of Urban Pollutant Conversion, Institute of Urban Environment, Chinese Academy of Sciences, Xiamen 361021, China

2. Research Center for Eco-Environmental Sciences, Chinese Academy of Sciences, Beijing 100085, China

3. University of Chinese Academy of Sciences, Beijing 100049, China

ARTICLE INFO

Article history:

Received 27 September 2018

Revised 21 November 2018

Accepted 22 November 2018

Available online 13 December 2018

Keywords:

NH₃-SCR

CeO₂

Acidity

Redox capability

H₂SO₄

ABSTRACT

The effect of acidity and redox capability over sulfuric acid-modified CeO₂ catalysts were studied for the selective catalytic reduction of NO_x with NH₃ (NH₃-SCR). The deposition of sulfate significantly enhanced the catalytic performance over CeO₂. NO_x conversion over 4H₂SO₄/CeO₂ at 230–440 °C was higher than 90%. The strong redox capability of CeO₂ could result in unselective NH₃ oxidation and decrease high temperatures catalytic activity and N₂ selectivity. The deposition of sulfate increased the acidity and weakened the redox capability, and then increased the high temperature NO_x conversion and N₂ selectivity. An appropriate level of acidity also promoted the activity at 190–250 °C over ceria-based catalysts, and with further increase in the acidity, the SCR activity decreased slightly. Weak redox capability lowered the low-temperature catalytic activity. Excellent SCR activity requires a balance of acidity and redox capability on the catalysts.

© 2018 The Research Center for Eco-Environmental Sciences, Chinese Academy of Sciences.

Published by Elsevier B.V.

Introduction

Nitrogen oxides are important atmospheric pollutants, contributing to serious environmental problems (Bosch and Janssen, 1988; Qi et al., 2004). The selective catalytic reduction of NO_x with NH₃ (NH₃-SCR) over V₂O₅-WO₃(MoO₃)/TiO₂ has been widely applied to remove NO_x (Bosch and Janssen, 1988; Busca et al., 2005). However, the vanadia-based catalysts still presented several disadvantages, such as the toxicity and volatility of V₂O₅ species, the narrow operating temperature window, high conversion of SO₂ to SO₃ and low N₂ selectivity at high temperatures (Balle et al., 2009; Busca et al., 1998; Dunn et al., 1998; Zhu et al., 2018). Consequently, the development of

new non-vanadia based catalysts with excellent catalytic performance is of great urgency.

Cerium oxide (CeO₂) has attracted a lot of interests due to the excellent redox properties and strong oxygen storage capability (Boningari et al., 2015; Duan et al., 2018; Wang et al., 2015; Weng et al., 2016; Zhao et al., 2017). Some CeO₂-based catalysts, such as CeO₂-TiO₂ (Shan et al., 2012), CeWO_x (Chen et al., 2011; Shan et al., 2015), Co-CeTi (Liu et al., 2017b) and Zr-CeVO₄ (Zhao et al., 2016), have shown good NH₃-SCR performance. The acidity of CeO₂ catalysts was found to be significantly enhanced by the introduction of tungstate (Chen et al., 2010), niobate (Qu et al., 2013), and sulfate (Zhang et al., 2016a), and which then increased the catalytic activity. The enhanced catalytic performance over

* Corresponding authors. E-mail: honghe@rcees.ac.cn, (Hong He), qcfeng@rcees.ac.cn. (Qingcai Feng).

H₃PO₄-modified CeO₂ was due to the reduction in redox ability and the increase in acidic strength (Yi et al., 2016). The interaction between phosphotungstic acid and CeO₂ contributed to excellent redox properties and favored the surface acidity of phosphotungstic acid-modified CeO₂ catalysts (Song et al., 2017). CeO₂ pretreated with different acids (HCl, HNO₃, HAc, H₂SO₄ and H₃PO₄) was studied, and the sample pretreated by H₂SO₄ was found to exhibit the best catalytic performance (Yao et al., 2017). The 2.5 wt.% SO₄²⁻/CeO₂ catalysts showed the highest catalytic activity and strong resistance to SO₂ and H₂O (Zhang et al., 2016b). Based on the above discussion, it is noteworthy that the NH₃-SCR activity over ceria-based catalysts could be improved by enhancing surface acidity. However, the relationship of SCR performance and the coupling of redox capability and acidity has not been investigated in depth for ceria-based catalysts.

In this study, acid modification of CeO₂ was conducted to study the coupling of acidity and redox capability of ceria-based catalysts. The CeO₂ catalyst was firstly synthesized via a hydrothermal route and then modified by H₂SO₄ using an impregnation method. The xH₂SO₄/CeO₂ catalyst showed excellent NH₃-SCR activity and strong resistance to H₂O and SO₂, due to the balance of acidity and redox capability.

1. Materials and methods

1.1. Catalyst synthesis

The CeO₂ sample was synthesized by a hydrothermal method. First we dissolved Ce(NO₃)₄ and NaOH in deionized water, respectively and then mixed them to obtain a purple slurry. Subsequently it was transferred into a Teflon-lined stainless-steel autoclave at 120°C and held there for 12 hr. The deionized water and anhydrous ethanol were used to wash the fresh precipitates for removing any possible ionic remnants. Finally, the sample was dried at 60°C overnight and calcined in static air at 550°C for 4 hr.

Sulfuric acid-modified CeO₂ catalysts were prepared via an impregnation route. H₂SO₄ solutions with different concentrations were added to the CeO₂ carrier. After stirring, the mixtures were desiccated at 110°C overnight and calcined in static air at 500°C for 3 hr. The catalysts were designated as xH₂SO₄/CeO₂, where x = 1, 2 and 4 represent the SO₄²⁻ loadings of 7.5, 15 and 30 wt.% added in the process of preparation, respectively. The surface composition of ceria-based catalysts as determined by XPS is present in Table S1 in Supporting Information. Different amounts of sulfur existed in xH₂SO₄/CeO₂ and sulfur mainly existed on the surface.

1.2. Characterization

A Quantachrome Autosorb iQ2 automatic adsorption instrument was applied to measure Nitrogen adsorption/desorption isotherms at -196°C. The samples were degassed at 300°C for 5 hr prior to N₂ physisorption. Surface area and pore structure were determined by the BET equation in the 0.05–0.30 partial pressure range and the Barrett-Joyner-Halenda (BJH) method from the desorption branches of the isotherms, respectively.

Powder XRD measurements were performed by a PANalytical B.V. X'Pert Pro XRD diffractometer using Cu K α radiation at

40 mA and 40 kV. The 2 θ data from 10 to 80° were recorded at 8°/min with the step size of 0.07°.

H₂-TPR experiments were conducted using a Quantachrome ChemStar analyzer. The samples (100 mg) were pretreated in Ar flow (100 ml/min) at 400°C for 30 min and then cooled down to 30°C followed by Ar purging. The reduction temperature was raised to 900°C at 10°C/min in H₂ (5 vol%)/Ar (100 ml/min).

O₂-TPD experiments were carried out on Micromeritics AutoChem 2920 Chemisorption Analyzer. A 100 mg sample was pretreated in He flow at 300°C for 30 min. The sample was then saturated with 5% O₂/He (50 ml/min) for 1 hr at 30°C and purged with He flow for 40 min. Finally, the sample was heated to 1000°C at the rate of 10°C/min in He flow (50 ml/min). The outlet exhaust was detected by TCD.

X-ray photoelectron spectroscopy (XPS) measurements were carried out on a PHI Quantum 2000 Scanning ESCA Microprobe with a monochromatized microfocused Al X-ray source. All the binding energies were calibrated using C1s as the reference energy (C1s = 284.6 eV).

1.3. In situDRIFTS studies

In situDRIFTS experiments were conducted on an FTIR spectrometer (Thermo Fisher Nicolet iS50) equipped with a Smart Collector and an MCT/A detector cooled by liquid nitrogen. The sample was pretreated in a flow of 20 vol.% O₂/N₂ at 300°C for 30 min, then cooled down to 225°C, and subsequently purged with N₂ for background collection. The reaction conditions were controlled as follows: 300 ml/min total flow rate, 500 ppm NH₃ or 500 ppm NO + 5 vol.% O₂ and N₂ balance. All spectra were recorded by accumulating 100 scans with a resolution of 4 cm⁻¹.

1.4. Activity tests

The NH₃-SCR activity tests over the ceria-based catalysts (40–60 mesh) were conducted in a fixed-bed quartz flow reactor. The inlet gases included 500 ppm NH₃ or/and 500 ppm NO, 5 vol.% O₂, 100 ppm SO₂ (when used), 10% H₂O (when used) and N₂ balance and GHSV 50,000 hr⁻¹. The effluent gases, including NH₃, NO, N₂O and NO₂, were analyzed by an FTIR gas analyzer (Thermo Fisher IGS).

2. Results

2.1. Catalyst characterization

2.1.1. BET and XRD results

The surface area and pore characterization results for ceria-based samples are shown in Table 1. The loading of sulfate on three xH₂SO₄/CeO₂ samples decreased the specific surface area and pore volume in all cases.

Fig. 1 presents the XRD results of ceria-based catalysts. The main peaks were assigned to CeO₂ with the cubic fluorite structure (43–1002) for all samples. The intensity of diffraction peaks for xH₂SO₄/CeO₂ catalysts was weaker than that of CeO₂, illustrating a loss of crystallinity. Due to the coverage and blockage of pores by sulfates, the specific surface area and crystallinity both decreased in the following sequence:

Table 1 – N₂ physisorption results of ceria-based catalysts.

Catalysts	Specific surface area (m ² /g)	Pore diameter (nm)	Pore volume (cm ³ /g)
CeO ₂	84.39	32.55	0.69
1H ₂ SO ₄ /CeO ₂	38.20	22.33	0.24
2H ₂ SO ₄ /CeO ₂	29.63	25.07	0.21
4H ₂ SO ₄ /CeO ₂	32.14	51.52	0.41

CeO₂ > 1H₂SO₄/CeO₂ > 2H₂SO₄/CeO₂. In addition, low intensity diffraction peaks ascribed to Ce₂(SO₄)₃ (27–0573), Ce(SO₄)₂ (70–2097) and CeOSO₄ (39–0515) were observed for the 4H₂SO₄/CeO₂ catalyst, indicating the existence of sulfates. The formation of new crystalline phases led to the slightly greater surface area and stronger crystallinity of 4H₂SO₄/CeO₂ than 2H₂SO₄/CeO₂. No peaks due to sulfate species were observed over 1H₂SO₄/CeO₂ and 2H₂SO₄/CeO₂, which could be due to the small quantity of sulfate species in these samples.

2.1.2. H₂-TPR and O₂-TPD results

H₂-TPR experiments was conducted to study the redox properties of ceria-based catalysts and the results are exhibited in Fig. 2a. According to the literature (Lian et al., 2015; Peng et al., 2012), the reduction peaks between 300 and 550°C and between 700 and 900°C for the CeO₂ catalyst can be attributed to the reduction of surface Ce⁴⁺ to Ce³⁺ and bulk Ce⁴⁺ to Ce³⁺, respectively. A distinctive H₂ reduction peak at 550–650°C was detected over xH₂SO₄/CeO₂, which was mainly assigned to the reduction of sulfate (Lian et al., 2017; Yang et al., 2013), due to the fact that the H₂ consumption of Ce⁴⁺ was small. It indicates that the catalyst was covered with a substantial amount of sulfate species. With increased sulfate loading on the catalysts, the reduction temperature became higher and the amount of H₂ consumption was larger. Although the amount of reducible species was larger, the reduction temperature for xH₂SO₄/CeO₂ was much higher than for CeO₂. The active temperature window in the NH₃-SCR reaction was below 500°C. In this temperature range CeO₂ presented stronger redox capability than xH₂SO₄/CeO₂.

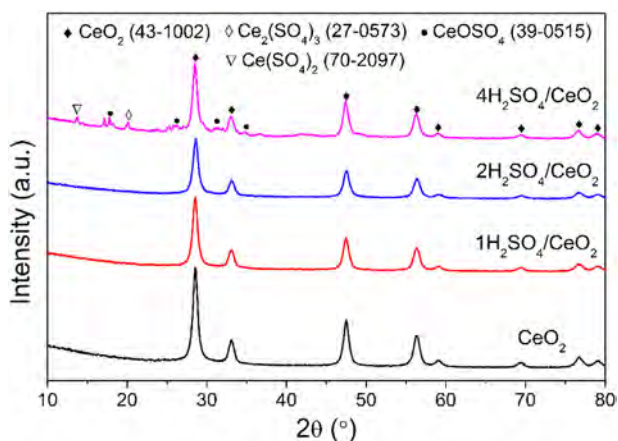


Fig. 1 – XRD patterns of ceria-based catalysts.

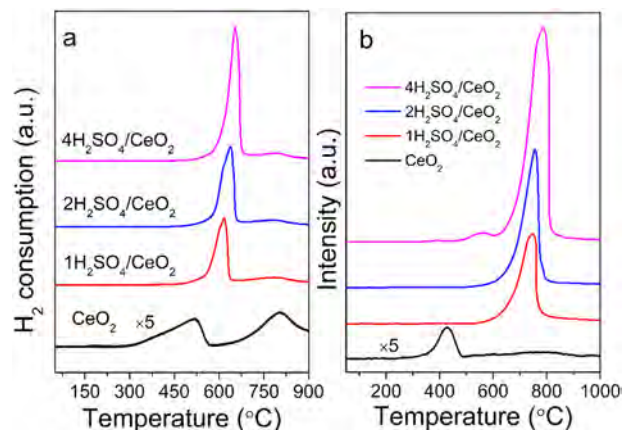


Fig. 2 – H₂-TPR profiles (a) and O₂-TPD results (b) of CeO₂ and acid-modified CeO₂ catalysts.

O₂-TPD results are shown in Fig. 2b. An O₂ desorption peak (β) centered at 425°C appears on CeO₂. As for acid-modified samples, a distinct desorption peak (γ) is observed in the temperature range of 600–800°C. The β and γ desorption peak are attributed to the oxygen-vacancy adsorbed oxygen and O²⁻ stripped from lattice oxygen sites, respectively (Ma et al., 2015; Sui et al., 2017). The desorption of surface active oxygen at low temperature indicated that CeO₂ provides a better oxidation environment for NH₃-SCR of NO than acid-modified samples.

2.1.3. XPS results

The ceria-based catalysts were studied by XPS to understand the chemical states of oxygen present on the surface. Fig. 3 shows the XPS of O 1s signals. The primary peaks at 528–532 eV were attributed to the lattice oxygen species (denoted as O_β) and the additional shoulder peaks at 532–535 eV were assigned to the surface oxygen species (denoted as O_α) (Andreoli et al., 2015; Liu et al., 2017a). The relative surface concentration ratios of O_α/O_{all} for the ceria-based catalysts

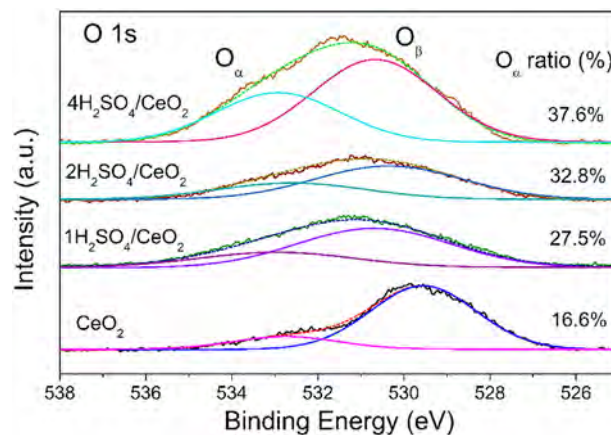


Fig. 3 – XPS O 1s results of CeO₂ and acid-modified CeO₂ catalysts.

were also listed in Fig. 3. The O_{α} ratios increased in the following order: $CeO_2 < 1H_2SO_4/CeO_2 < 2H_2SO_4/CeO_2 < 4H_2SO_4/CeO_2$. This indicated that there is more abundant surface oxygen on xH_2SO_4/CeO_2 , which is possibly due to the contribution of surface SO_4^{2-} . The results were in good accordance with the H_2 -TPR results, which show the presence of more reducible species on xH_2SO_4/CeO_2 . However, the oxygen species from surface SO_4^{2-} presented low oxidation activity, from the H_2 -TPR results.

The XPS spectra in Ce 3d region and the relative ratio of Ce^{3+} are shown in Fig. S1. The surface Ce^{3+} ratio on CeO_2 was higher than acid-modified catalysts, which could favor to the formation of surface active oxygen. Therefore, CeO_2 presents stronger redox capability, which is in accordance with the results of O_2 -TPD.

2.2. In situ DRIFTS

Fig. 4a presents the DRIFT spectra of NH_3 adsorption on CeO_2 and acid-modified CeO_2 catalysts at 225 °C. The surface of the catalysts were covered by several different ammonia species after NH_3 adsorption. The peaks at 1432 cm^{-1} were ascribed to the bending vibrations of NH_4^+ on Brønsted acid sites (Liu et al., 2017b; Yu et al., 2017; Zhang and Hou, 2016). The bands assigned to N-H stretching vibration region of coordinated NH_3 on Lewis acid sites were also observed at 3390, 3260 and 3157 cm^{-1} (Ma et al., 2016; Zhang et al., 2015b). The negative band at 1362 cm^{-1} on xH_2SO_4/CeO_2 derived from the coverage of sulfate species by NH_3 , while the coverage or hydration of part of the residual sulfate species by H_2O resulted in the negative band at 1385 cm^{-1} (Liu et al., 2011). The amount of acid sites increased in the following sequence: $CeO_2 < 1H_2SO_4/CeO_2 < 2H_2SO_4/CeO_2 < 4H_2SO_4/CeO_2$, indicating that the acidity on CeO_2 surface was significantly improved by H_2SO_4 modification, including Lewis acid sites and Brønsted acid sites. The NH_3 -TPD results also indicated more acid sites of $1H_2SO_4/CeO_2$ than that of CeO_2 (Fig. S2).

DRIFT spectra of $NO + O_2$ adsorption on ceria-based catalysts at 225 °C are shown in Fig. 4b. When CeO_2 was exposed to $NO + O_2$, several bands attributed to nitrate

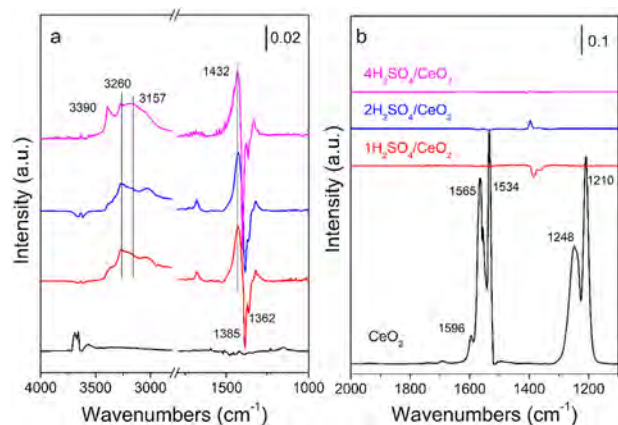


Fig. 4 – DRIFTS of NH_3 adsorption (a) and $NO + O_2$ adsorption (b) on ceria-based catalysts at 225 °C.

species were detected, including bridging nitrate (1210 and 1596 cm^{-1}), bidentate nitrate (1565 and 1248 cm^{-1}) and monodentate nitrate (1534 cm^{-1}) (Ma et al., 2016; Zhang et al., 2015a). There were no nitrate species adsorbed on xH_2SO_4/CeO_2 , in accordance with the NO -TPD results (Fig. S3). The formation of nitrate might be inhibited by the strong acidity of xH_2SO_4/CeO_2 .

To study the reactivity of adsorbed ammonia species in NH_3 -SCR reaction on $4H_2SO_4/CeO_2$, in situ DRIFTS of the reaction between $NO + O_2$ and pre-adsorbed NH_3 at 225 °C were recorded as a function of time (Fig. 5a). The surface was covered with several adsorbed ammonia species after exposure to NH_3 . When introducing $NO + O_2$, we can see that the peaks attributed to adsorbed NH_3 species diminished gradually. One band ascribed to H_2O at 1612 cm^{-1} (Lian et al., 2017) was detected at the same time. No nitrate species or other nitrogenous intermediates were observed on the surface during the whole reaction process, indicating an Eley-Rideal reaction mechanism between gaseous or weakly adsorbed NO and adsorbed NH_3 species.

The above results exhibited that no adsorbed NO_x species formed on $4H_2SO_4/CeO_2$, in good accordance with the results shown in Fig. 5b. No bands assigned to adsorbed NO_x species were observed after $NO + O_2$ adsorption at 225 °C. When ammonia was introduced, bands attributed to NH_3 adsorbed species were detected, including ionic NH_4^+ on Brønsted acid sites (1432 cm^{-1}) and N-H stretching vibration bands from coordinated NH_3 (3390 , 3260 and 3157 cm^{-1}). The results indicated that the reaction between adsorbed NO_x species and adsorbed NH_3 species did not occur. Therefore, the NH_3 -SCR reaction over the $4H_2SO_4/CeO_2$ catalyst mainly followed the Eley-Rideal mechanism, similar to the CeO_2 -HF catalyst in literature (Yang et al., 2016).

2.3. Catalytic performance

NO_x conversion over the ceria-based catalysts is exhibited in Fig. 6a. The CeO_2 catalyst exhibited low activity, with a

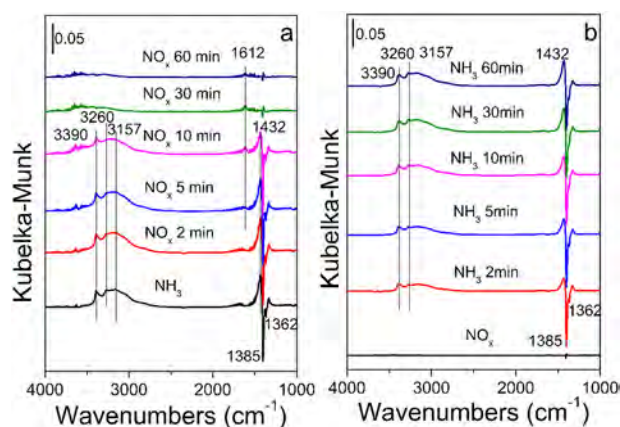


Fig. 5 – In situ DRIFT spectra of $4H_2SO_4/CeO_2$ pretreated by exposure to NH_3 followed by exposure to $NO + O_2$ (a) and pretreated by exposure to $NO + O_2$ followed by exposure to NH_3 (b) at 225 °C.

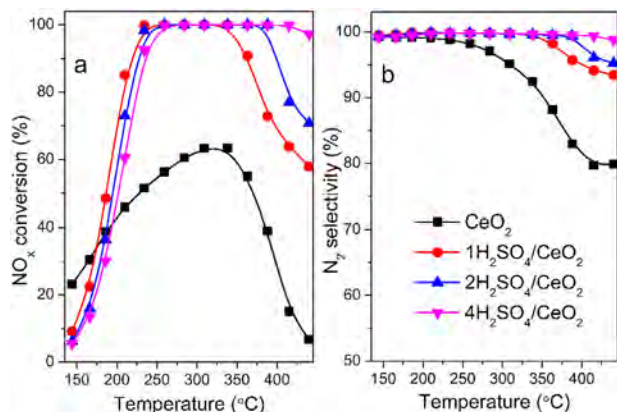


Fig. 6 – NO_x conversion (a) and N_2 selectivity (b) over ceria-based catalysts.

maximum NO_x conversion of 60% at 330°C. The modification of CeO_2 by H_2SO_4 led to a remarkable enhancement of NH_3 -SCR activity at 190–440°C. With further increase in the sulfate loading, NO_x conversion decreased a little at 190–250°C and was enhanced significantly at 250–440°C. $4\text{H}_2\text{SO}_4/\text{CeO}_2$ showed almost 100% NO_x conversion at 250–440°C. However, after the deposition of sulfate the catalytic activity over CeO_2 at 140–190°C decreased. The N_2 selectivity of ceria-based catalysts is exhibited in Fig. 6b. The N_2 selectivity increased with sulfate loading on the ceria-based catalysts. The three $x\text{H}_2\text{SO}_4/\text{CeO}_2$ catalysts all exhibited higher than 90% N_2 selectivity over the whole temperature range that we investigated. $4\text{H}_2\text{SO}_4/\text{CeO}_2$ also exhibited strong H_2O and SO_2 resistance (Fig. S4). The introduction of H_2SO_4 significantly boosted the catalytic performance of CeO_2 , including NO_x conversion at 190–440°C and N_2 selectivity.

2.4. NO and NH_3 oxidation activity

The separate oxidation activity of NO to NO_2 of the ceria-based catalysts was tested (Fig. 7a). CeO_2 presented the

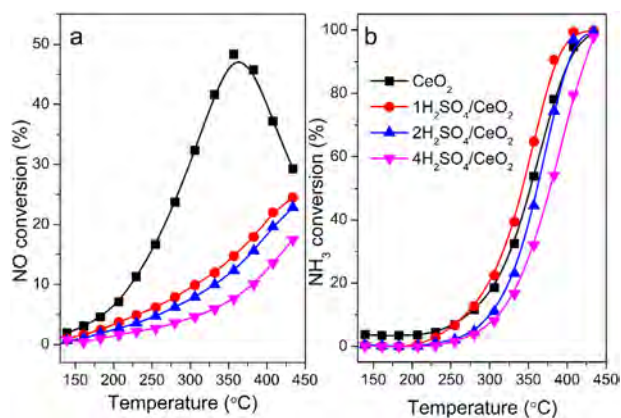


Fig. 7 – Separate NO oxidation activity (a) and separate NH_3 oxidation activity (b) over ceria-based catalysts.

highest NO oxidation activity. About 50% NO oxidation activity was obtained at 350°C and the oxidation activity decreased at higher temperature, in accordance with the thermodynamic limit (Wen et al., 2007). With the increase of sulfate loading, the NO oxidation activity decreased. The ammonia oxidation activity over ceria-based catalysts is exhibited in Fig. 7b. The separate NH_3 oxidation activity decreased in the following sequence: $1\text{H}_2\text{SO}_4/\text{CeO}_2 > 2\text{H}_2\text{SO}_4/\text{CeO}_2 > 4\text{H}_2\text{SO}_4/\text{CeO}_2$, similar to the NO oxidation activity. CeO_2 shows similar NH_3 oxidation activity to that of $2\text{H}_2\text{SO}_4/\text{CeO}_2$. However, the NH_3 oxidation over CeO_2 produced large amounts of NO , NO_2 and N_2O , compared with $x\text{H}_2\text{SO}_4/\text{CeO}_2$ (Fig. 8). The high temperature activity and N_2 selectivity decreased due to the over-oxidation of NH_3 over CeO_2 . CeO_2 showed high NO oxidation activity but low NH_3 oxidation activity, which will be discussed in detail later.

3. Discussion

The modification of CeO_2 by H_2SO_4 significantly enhanced the NH_3 -SCR activity at 190–440°C. With further increase in sulfate loading, NO_x conversion decreased slightly at low temperature (190–250°C) and increased at high temperature (250–440°C). The N_2 selectivity also increased with the sulfate loading on the catalysts.

Previous studies have shown that at low temperatures the redox properties of a catalyst are the key factors governing the reactivity, while at high temperatures the surface acidity plays a crucial role in the NH_3 -SCR reaction (Li et al., 2008; Lietti, 1996; Liu et al., 2006). From the H_2 -TPR results, the onset temperature of H_2 reduction for CeO_2 was much lower than that of $x\text{H}_2\text{SO}_4/\text{CeO}_2$. CeO_2 presented much stronger redox capability at low temperature than the sulfate-modified CeO_2 catalysts. Therefore, CeO_2 showed the highest NO oxidation activity. NH_3 oxidation over CeO_2 produced large amounts of N_2O , NO and NO_2 , leading to the decrease of NO_x conversion and N_2 selectivity at high temperature. The deposition of sulfate increased the acidity and weakened the redox capability of the catalysts. As a result, the separate NH_3 oxidation and separate NO oxidation activities decreased with the increase of sulfate loading. Therefore, NO_x conversion and N_2 selectivity increased at high temperature. At the same time, the weaker redox capability at low temperature resulted in lower NO_x conversion at 140–190°C for $x\text{H}_2\text{SO}_4/\text{CeO}_2$ than that for CeO_2 .

However, redox capability and acidity are both essential for SCR over ceria-based catalysts in the middle temperature range, such as 190–250°C. From the DRIFTS results, the deposition of sulfate strongly enhanced the acidity of CeO_2 . The presence of more acid sites favors the adsorption and activation of ammonia in NH_3 -SCR reaction and then enhances the catalytic performance. Therefore, the low-temperature NO_x conversion of CeO_2 at 190–250°C was boosted notably after modification by sulfate. However, further increase in acidity led to a decline in the redox capability based on H_2 -TPR results, and the activity also decreased slightly.

Though CeO_2 showed high NO oxidation activity, NH_3 oxidation activity was low. This might be due to the fact that

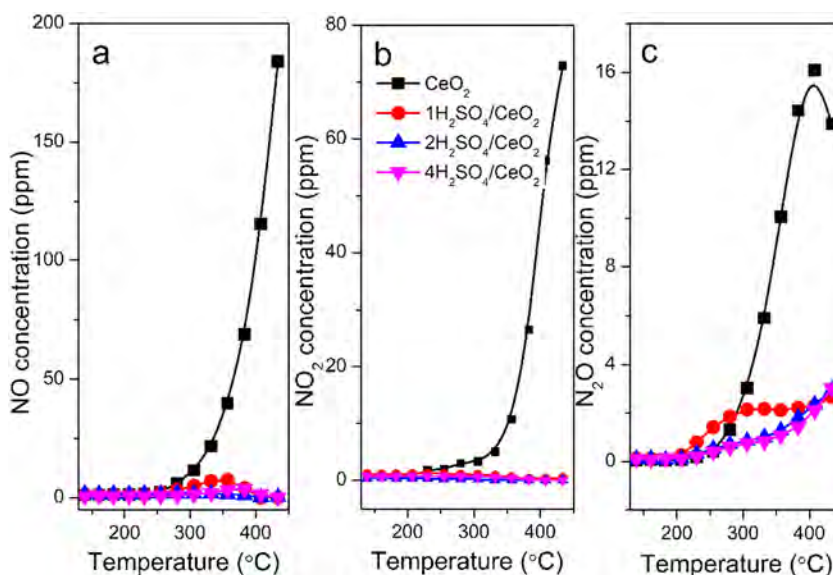


Fig. 8 – The products of separate NH_3 oxidation (Fig. 7b) over ceria-based catalysts.

CeO_2 has weak acidity and cannot adsorb and activate NH_3 effectively.

Strong redox capability could lead to the over-oxidation of NH_3 and decrease the NO_x conversion and N_2 selectivity at high temperature. Strong acidity could enhance the catalytic activity and reduce the over-oxidation of NH_3 . However, an excess of acid sites might cover part of the redox sites and result in a decrease in the low temperatures catalytic activity. Achieving appropriate redox capability and acidity simultaneously will result in an excellent NH_3 -SCR catalyst.

4. Conclusions

To study the influence of the acidity and redox capability, CeO_2 catalysts were modified by H_2SO_4 using an impregnation method for the selective catalytic reduction of NO_x by NH_3 . A series of $x\text{H}_2\text{SO}_4/\text{CeO}_2$ catalysts all showed significantly better NH_3 -SCR performance than CeO_2 at 190–440°C. CeO_2 , with strong redox capability, showed low NO_x conversion and N_2 selectivity at high temperature. With the increase of acidity, the high temperature activity and N_2 selectivity increased at 250–440°C. The appropriate level of acidity also enhanced the NH_3 -SCR activity at 190–250°C. Too much acid sites could weaken the redox capability and decrease the catalytic activity slightly at low temperature. The proper balance of acidity and redox capability will result in an excellent NH_3 -SCR catalyst. The NH_3 -SCR reaction over $4\text{H}_2\text{SO}_4/\text{CeO}_2$ mainly followed the Eley-Rideal mechanism, in which adsorbed NH_3 species reacted with gaseous or weakly adsorbed NO to finally form N_2 and H_2O .

Acknowledgements

This work was financially supported by National Key R&D Program of China (No. 2016YFC0205301), the Key Project of National Natural Science Foundation (No. 21637005), the

National Natural Science Foundation of China (No. 21607149) and the Natural Science Foundation of Fujian Province, China (No. 2016J05142).

Appendix A. Supplementary data

Supplementary data to this article can be found online at <https://doi.org/10.1016/j.jes.2018.11.018>.

REFERENCES

- Andreoli, S., Deorsola, F.A., Pirone, R., 2015. MnO_x - CeO_2 catalysts synthesized by solution combustion synthesis for the low-temperature NH_3 -SCR. *Catal. Today* 253, 199–206.
- Balle, P., Geiger, B., Kureti, S., 2009. Selective catalytic reduction of NO_x by NH_3 on Fe/HBEA zeolite catalysts in oxygen-rich exhaust. *Appl. Catal. B-environ.* 85, 109–119.
- Bonngari, T., Pappas, D.K., Ettireddy, P.R., Kotrba, A., Smirniotis, P. G., 2015. Influence of SiO_2 on M/TiO_2 ($\text{M} = \text{Cu}, \text{Mn}, \text{and Ce}$) formulations for low-temperature selective catalytic reduction of NO_x with NH_3 : surface properties and key components in relation to the activity of NO_x reduction. *Ind. Eng. Chem. Res.* 54, 2261–2273.
- Bosch, H., Janssen, F., 1988. Formation and control of nitrogen oxides. *Catal. Today* 2, 369–379.
- Busca, G., Lietti, L., Ramis, G., Berti, F., 1998. Chemical and mechanistic aspects of the selective catalytic reduction of NO_x by ammonia over oxide catalysts: a review. *Appl. Catal. B-Environ.* 18, 1–36.
- Busca, G., Larrubia, M.A., Arrighi, L., Ramis, G., 2005. Catalytic abatement of NO_x : Chemical and mechanistic aspects. *Catal. Today* 107–108, 139–148.
- Chen, L., Li, J., Ge, M., Zhu, R., 2010. Enhanced activity of tungsten modified $\text{CeO}_2/\text{TiO}_2$ for selective catalytic reduction of NO_x with ammonia. *Catal. Today* 153, 77–83.
- Chen, L., Li, J., Ablikim, W., Wang, J., Chang, H., Ma, L., et al., 2011. CeO_2 - WO_3 mixed oxides for the selective catalytic reduction of NO_x by NH_3 over a wide temperature range. *Catal. Lett.* 141, 1859–1864.

- Duan, Z., Liu, J., Shi, J., Zhao, Z., Wei, Y., Zhang, X., et al., 2018. The selective catalytic reduction of NO over Ce_{0.3}TiO_x-supported metal oxide catalysts. *J. Environ. Sci.* 65, 1–7.
- Dunn, J., Koppula, P., Stenger, H., Wachs, I., 1998. Oxidation of sulfur dioxide to sulfur trioxide over supported vanadia catalysts. *Appl. Catal. B-Environ.* 19, 103–117.
- Li, Y., Cheng, H., Li, D., Qin, Y., Xie, Y., Wang, S., 2008. WO₃/CeO₂-ZrO₂, a promising catalyst for selective catalytic reduction (SCR) of NO_x with NH₃ in diesel exhaust. *Chem. Commun.* 1470–1472.
- Lian, Z., Liu, F., He, H., 2015. Effect of preparation methods on the activity of VO_x/CeO₂ catalysts for the selective catalytic reduction of NO_x with NH₃. *Catal. Sci. Technol.* 5, 389–396.
- Lian, Z., Liu, F., Shan, W., He, H., 2017. Improvement of Nb doping on SO₂ resistance of VO_x/CeO₂ catalyst for the selective catalytic reduction of NO_x with NH₃. *J. Phys. Chem. C* 121, 7803–7809.
- Lietti, L., 1996. Reactivity of V₂O₅-WO₃/TiO₂ de-NO_x catalysts by transient methods. *Appl. Catal. B-Environ.* 10, 281–297.
- Liu, Q., Liu, Z., Li, C., 2006. Adsorption and activation of NH₃ during selective catalytic reduction of NO by NH₃. *Chin. J. Catal.* 27, 636–646.
- Liu, F., Asakura, K., He, H., Shan, W., Shi, X., Zhang, C., 2011. Influence of sulfation on iron titanate catalyst for the selective catalytic reduction of NO_x with NH₃. *Appl. Catal. B-Environ.* 103, 369–377.
- Liu, J., Li, G.Q., Zhang, Y.F., Liu, X.Q., Wang, Y., Li, Y., 2017a. Novel Ce-W-Sb mixed oxide catalyst for selective catalytic reduction of NO_x with NH₃. *Appl. Surf. Sci.* 401, 7–16.
- Liu, J., Li, X., Zhao, Q., Ke, J., Xiao, H., Lv, X., et al., 2017b. Mechanistic investigation of the enhanced NH₃-SCR on cobalt-decorated Ce-Ti mixed oxide: in situ FTIR analysis for structure-activity correlation. *Appl. Catal. B-Environ.* 200, 297–308.
- Ma, Z., Wu, X., Si, Z., Weng, D., Ma, J., Xu, T., 2015. Impacts of niobia loading on active sites and surface acidity in NbO_x/CeO₂-ZrO₂ NH₃-SCR catalysts. *Appl. Catal. B-Environ.* 179, 380–394.
- Ma, Z., Wu, X., Harelind, H., Weng, D., Wang, B., Si, Z., 2016. NH₃-SCR reaction mechanisms of NbO_x/Ce_{0.75}Zr_{0.25}O₂ catalyst: DRIFTS and kinetics studies. *J. Mol. Catal. A-Chem.* 423, 172–180.
- Peng, Y., Li, J.H., Chen, L., Chen, J.H., Han, J., Zhang, H., et al., 2012. Alkali metal poisoning of a CeO₂-WO₃ catalyst used in the selective catalytic reduction of NO_x with NH₃: an experimental and theoretical study. *Environ. Sci. Technol.* 46, 2864–2869.
- Qi, G.S., Yang, R.T., Chang, R., 2004. MnO_x-CeO₂ mixed oxides prepared by co-precipitation for selective catalytic reduction of NO with NH₃ at low temperatures. *Appl. Catal. B-Environ.* 51, 93–106.
- Qu, R., Gao, X., Cen, K., Li, J., 2013. Relationship between structure and performance of a novel cerium-niobium binary oxide catalyst for selective catalytic reduction of NO with NH₃. *Appl. Catal. B-Environ.* 142–143, 290–297.
- Shan, W., Liu, F., He, H., Shi, X., Zhang, C., 2012. An environmentally-benign CeO₂-TiO₂ catalyst for the selective catalytic reduction of NO_x with NH₃ in simulated diesel exhaust. *Catal. Today* 184, 160–165.
- Shan, W., Liu, F., Yu, Y., He, H., Deng, C., Zi, X., 2015. High-efficiency reduction of NO_x emission from diesel exhaust using a CeWO_x catalyst. *Catal. Commun.* 59, 226–228.
- Song, Z., Zhang, Q., Ma, Y., Liu, Q., Ning, P., Liu, X., et al., 2017. Mechanism-dependent on the different CeO₂ supports of phosphotungstic acid modification CeO₂ catalysts for the selective catalytic reduction of NO with NH₃. *J. Taiwan Inst. Chem. Eng.* 71, 277–284.
- Sui, G., Xue, Z., Zhou, D., Wang, Y., Shen, Y., Zong, Y., et al., 2017. The influence factors on CeSn_{0.8}W_{0.6}O_x/TiO₂ for catalytic removals of NO, CO and C₃H₈. *J. Ind. Eng. Chem.* 51, 229–236.
- Wang, J., Dong, X., Wang, Y., Li, Y., 2015. Effect of the calcination temperature on the performance of a CeMoO_x catalyst in the selective catalytic reduction of NO_x with ammonia. *Catal. Today* 245, 10–15.
- Wen, Y., Zhang, C., He, H., Yu, Y., Teraoka, Y., 2007. Catalytic oxidation of nitrogen monoxide over La_{1-x}Ce_xCoO₃ perovskites. *Catal. Today* 126, 400–405.
- Weng, X., Dai, X., Zeng, Q., Liu, Y., Wu, Z., 2016. DRIFT studies on promotion mechanism of H₃PW₁₂O₄₀ in selective catalytic reduction of NO with NH₃. *J. Colloid Interface Sci.* 461, 9–14.
- Yang, S.J., Guo, Y.F., Chang, H.Z., Ma, L., Peng, Y., Qu, Z., et al., 2013. Novel effect of SO₂ on the SCR reaction over CeO₂: mechanism and significance. *Appl. Catal. B-Environ.* 136, 19–28.
- Yang, N., Guo, R., Tian, Y., Pan, W., Chen, Q., Wang, Q., et al., 2016. The enhanced performance of ceria by HF treatment for selective catalytic reduction of NO with NH₃. *Fuel* 179, 05–311.
- Yao, X., Wang, Z., Yu, S., Yang, F., Dong, L., 2017. Acid pretreatment effect on the physicochemical property and catalytic performance of CeO₂ for NH₃-SCR. *Appl. Catal. A-Gen.* 542, 282–288.
- Yi, T., Zhang, Y., Li, J., Yang, X., 2016. Promotional effect of H₃PO₄ on ceria catalyst for selective catalytic reduction of NO by NH₃. *Chin. J. Catal.* 37, 300–307.
- Yu, Y., Miao, J., Wang, J., He, C., Chen, J., 2017. Facile synthesis of CuSO₄/TiO₂ catalysts with superior activity and SO₂ tolerance for NH₃-SCR: physicochemical properties and reaction mechanism. *Catal. Sci. Technol.* 7, 1590–1601.
- Zhang, P., Hou, Q.Z., 2016. SnO₂ modified Ce-Ti-O-x catalyst for the selective catalytic reduction of NO_x with NH₃. *React. Kinet. Mech. Cat.* 117, 119–128.
- Zhang, L., Li, L., Cao, Y., Xiong, Y., Wu, S., Sun, J., et al., 2015a. Promotional effect of doping SnO₂ into TiO₂ over a CeO₂/TiO₂ catalyst for selective catalytic reduction of NO by NH₃. *Catal. Sci. Technol.* 5, 2188–2196.
- Zhang, T., Qu, R., Su, W., Li, J., 2015b. A novel Ce-Ta mixed oxide catalyst for the selective catalytic reduction of NO_x with NH₃. *Appl. Catal. B-Environ.* 176, 338–346.
- Zhang, L., Qu, H.X., Du, T.Y., Ma, W.H., Zhong, Q., 2016a. H₂O and SO₂ tolerance, activity and reaction mechanism of sulfated Ni-Ce-La composite oxide nanocrystals in NH₃-SCR. *Chem. Eng. J.* 296, 122–131.
- Zhang, Q., Zhang, J., Song, Z., Ning, P., Li, H., Liu, X., 2016b. A novel and environmentally friendly SO₄²⁻/CeO₂ catalyst for the selective catalytic reduction of NO with NH₃. *J. Ind. Eng. Chem.* 34, 165–171.
- Zhao, X., Huang, L., Li, H.R., Hu, H., Hu, X.N., Shi, L.Y., et al., 2016. Promotional effects of zirconium doped CeVO₄ for the low-temperature selective catalytic reduction of NO_x with NH₃. *Appl. Catal. B-Environ.* 183, 269–281.
- Zhao, B., Ran, R., Guo, X., Cao, L., Xu, T., Chen, Z., et al., 2017. Nb-modified Mn/Ce/Ti catalyst for the selective catalytic reduction of NO with NH₃ at low temperature. *Appl. Catal. A-Gen.* 545, 64–71.
- Zhu, L., Zhong, Z., Xue, J., Xu, Y., Wang, C., Wang, L., 2018. NH₃-SCR performance and the resistance to SO₂ for Nb doped vanadium based catalyst at low temperatures. *J. Environ. Sci.* 65, 306–316.